Journal of Spatial Information Sciences

... JSIS



# HYBRID CNN–MLP DEEP LEARNING FRAMEWORK FOR URBAN LAND COVER MAPPING IN HETEROGENEOUS TROPICAL LANDSCAPES

Victor C Nnam, Uche H. Ikwueze, Gabrial J. Okon



JOURNAL OF SPATIAL INFORMATION SCIENCES ISSN: 2354-3361
VOL. 3, ISSUE 1, PP 34–62, 2026 DOI: https://doi.org/10.5281/zenodo.20705010
PUBLISHED 15-05-2026

www.journals.unizik.edu.ng/jsis

# HYBRID CNN–MLP DEEP LEARNING FRAMEWORK FOR URBAN LAND COVER MAPPING IN HETEROGENEOUS TROPICAL LANDSCAPES

**[1]Victor C Nnam, [2]Uche H. Ikwueze, [3]Gabrial J. Okon**

[1,2,3]Department of Geoinformatics and Surveying, University of Nigeria, Enugu Campus

Email: [1]victor.nnam@gmail.com, [2]jerryuc2@gmail.com, [3]okongabriel977@gmail.com

Phone: [1]+2348032760910, [2]+2347068659260, [3]+2348100434424

**DOI:** https://doi.org/10.5281/zenodo.20705010

## Abstract

Rapid urbanization in sub-Saharan Africa presents significant challenges for sustainable land management, particularly in tropical landscapes where spectral similarities between built-up areas and bare soil often lead to classification inaccuracies. While Convolutional Neural Networks (CNNs) have shown promise in remote sensing, they often struggle to resolve 'spectral confusion', a phenomenon where distinct land covers exhibit identical spectral signatures, because they prioritize spatial feature extraction over the non-linear spectral relationships required for class discrimination. To overcome these limitations, this study proposed a Hybrid Deep Learning framework that integrates a Multi-Layer Perceptron (MLP) with a CNN, combined with expert-driven spatial feature engineering. Using multi-temporal Landsat imagery (2000–2025) for Uyo Metropolis, Nigeria, the study developed a dual-stream architecture that fuses raw spectral bands with Center-Versus-Neighbors (CVN) texture descriptors and the Normalized Difference Vegetation Index (NDVI). The empirical findings demonstrated that the hybrid framework significantly outperforms traditional baseline classifiers (Random Forest), achieving a validated Overall Accuracy of 96.17% and a Kappa Coefficient of 0.94, calculated across the independent test set. The inclusion of spatial texture successfully resolved spectral confusion, reducing misclassification of "Bare Land" as "Built-up" by 22%. Spatiotemporal analysis revealed a 158.10% increase in the urban footprint over the 25-year period, with the most aggressive expansion (3.95 km²/year) occurring between 2020 and 2025. The study concluded that hybrid architectures are essential for mapping heterogeneous tropical environments. The proposed framework offers a scalable, high-precision, and low-cost tool for monitoring urban sprawl in secondary African cities, providing a robust empirical foundation for achieving Sustainable Development Goal (SDG) 11 targets.

**Keywords:** Deep Learning; Hybrid CNN-MLP; Urban Expansion; LULC Classification; Uyo Metropolis; Feature Engineering; Remote Sensing

JOURNAL OF SPATIAL INFORMATION SCIENCES ISSN: 2354-3361
VOL. 3, ISSUE 1, PP 34–62, 2026 DOI: https://doi.org/10.5281/zenodo.20705010
PUBLISHED 15-05-2026
www.journals.unizik.edu.ng/jsis

## Introduction

Rapid urbanization has become one of the defining global trends of the twenty-first century. Currently, more than 55% of the world's population resides in urban areas, a proportion projected to increase to approximately 68% by 2050 [1]. A substantial share of this growth is occurring in sub-Saharan Africa, where expanding urban populations are driving extensive land transformation, often in the absence of effective planning frameworks [2]. Such rapid urban expansion places significant pressure on infrastructure, natural resources, and environmental systems, thereby creating an urgent need for sustainable urban management strategies. Consequently, accurate monitoring of Land Use and Land Cover (LULC) dynamics has become essential for urban planning, environmental management, and informed decision-making [3].

Reliable LULC classification forms the foundation for understanding urban growth patterns and assessing landscape change. However, mapping urban environments remains particularly challenging in tropical regions characterized by heterogeneous land-cover compositions. Built-up areas, bare soil, sparse vegetation, and other surface features frequently exhibit similar spectral responses, resulting in considerable classification uncertainty [3][4]. This phenomenon, commonly referred to as spectral confusion, often leads to misclassification when relying solely on spectral information. For example, bright concrete rooftops may exhibit reflectance characteristics similar to sandy or exposed soil surfaces, making it difficult for conventional classifiers to distinguish between these classes [5].

Traditionally, LULC mapping has relied on both parametric and non-parametric classification techniques, including Maximum Likelihood Classification (MLC), Random Forest (RF), and Support Vector Machines (SVM) [6] [7] [8]. While these approaches have demonstrated effectiveness across a range of applications, they primarily operate on a per-pixel basis and often fail to fully exploit the spatial and contextual information embedded within remotely sensed imagery. As a result, their performance tends to decline in complex urban landscapes where neighboring pixels and texture patterns provide critical information for distinguishing spectrally similar land-cover classes [9].

Recent advances in Deep Learning (DL) have significantly improved the capability of remote sensing systems to address these challenges. Unlike traditional machine learning algorithms, deep

learning models can automatically learn hierarchical feature representations from large datasets, enabling them to capture both spectral and spatial characteristics of land-cover classes. Among these approaches, Convolutional Neural Networks (CNNs) have emerged as particularly effective because of their ability to learn local spatial structures, texture patterns, and contextual relationships through convolutional operations [10] [11]. Studies have demonstrated that CNN-based approaches can substantially reduce spectral confusion and improve classification performance in heterogeneous urban environments. For instance, a research reported classification accuracies of up to 97.7% using Sentinel-2 imagery, highlighting the effectiveness of CNNs in distinguishing settlements from barren and fallow land despite their spectral similarity [12].

In addition to CNN-based approaches, transfer learning has further enhanced the applicability of deep learning for LULC classification. Rather than training networks from scratch, researchers have successfully adapted pre-trained architectures to remote sensing tasks. Naushad et al. (2021), for example, fine-tuned pre-trained Visual Geometry Group (VGG16) and Wide Residual Network (WRN) models using the EuroSAT dataset and achieved classification accuracies exceeding 99% [13]. These findings demonstrate the value of using learned representations and combining spectral, spatial, and textural information to improve classification robustness and accuracy.

Despite these advances, individual deep learning architectures still exhibit limitations. CNNs excel at extracting spatial and contextual information but may not fully preserve detailed spectral relationships. Conversely, Multi-Layer Perceptrons (MLPs) are effective at modeling complex non-linear spectral patterns but lack the ability to explicitly capture spatial dependencies [14] [15]. Consequently, the use of either architecture in isolation may limit classification performance in highly heterogeneous tropical urban environments where both spectral and spatial characteristics are equally important. Recent studies have therefore emphasized the need for hybrid architectures capable of integrating complementary feature representations to achieve greater robustness and classification accuracy [16].

Although hybrid deep learning approaches are increasingly gaining attention, a significant research gap remains in the development of integrated frameworks that simultaneously exploit spatial-textural and spectral information for LULC classification in tropical urban landscapes. Furthermore, relatively few studies have investigated the application of such frameworks for long-

term urban expansion monitoring in rapidly growing Nigerian cities. To address this gap, this study proposes a Hybrid CNN–MLP framework that integrates expert-derived spatial features, including Center-Versus-Neighbors (CVN) texture descriptors and the Normalized Difference Vegetation Index (NDVI), with raw spectral information to improve classification performance and minimize spectral confusion.

The specific objectives of this study are to:

a) Develop and evaluate a Hybrid CNN–MLP framework that integrates expert-derived spatial features (CVN texture and NDVI) with raw spectral bands to minimize spectral confusion.
b) Quantify and map the spatiotemporal urban expansion of Uyo Metropolis over the period 2000–2025, identifying key phases of urban growth.
c) Assess the performance and reliability of the proposed hybrid architecture relative to traditional classification approaches in a high-density tropical urban environment.

To achieve these objectives, the study seeks to answer the following research questions:

i. How does the integration of Center-Versus-Neighbors (CVN) texture descriptors enhance the ability of a deep learning framework to resolve spectral confusion between urban rooftops and bare soil compared with standalone CNN architectures?
ii. What are the primary temporal patterns and spatial characteristics of urban expansion within Uyo Metropolis between 2000 and 2025?
iii. To what extent does the proposed Hybrid CNN–MLP framework improve classification accuracy and reliability compared with traditional machine learning classifiers?

**Study Area**

The study is centered on Uyo, the capital city of Akwa Ibom State, located in the Niger Delta region of South-South Nigeria. Geographically, the area lies between latitudes 4°58' N and 5°05' N and longitudes 7°50' E and 8°00' E. The study area covers approximately 312 km², encompassing the rapidly urbanizing core and its transitioning peri-urban fringes [17] [18]. Uyo sits on a nearly level plain, with elevations ranging from 38 m to 105 m above sea level. This low-lying

JOURNAL OF SPATIAL INFORMATION SCIENCES ISSN: 2354-3361
VOL. 3, ISSUE 1, PP 34–62, 2026 DOI: https://doi.org/10.5281/zenodo.20705010
PUBLISHED 15-05-2026
www.journals.unizik.edu.ng/jsis

topography, combined with a tropical monsoon climate characterized by high annual rainfall (over 2,500 mm), results in a landscape dominated by dense rainforest fragments and oil palm bush. Since its designation as a state capital in 1987, Uyo has experienced an administrative and economic boom. This has triggered a massive influx of population and infrastructural development, leading to the conversion of vast tracts of secondary forest into residential and commercial built-up areas.

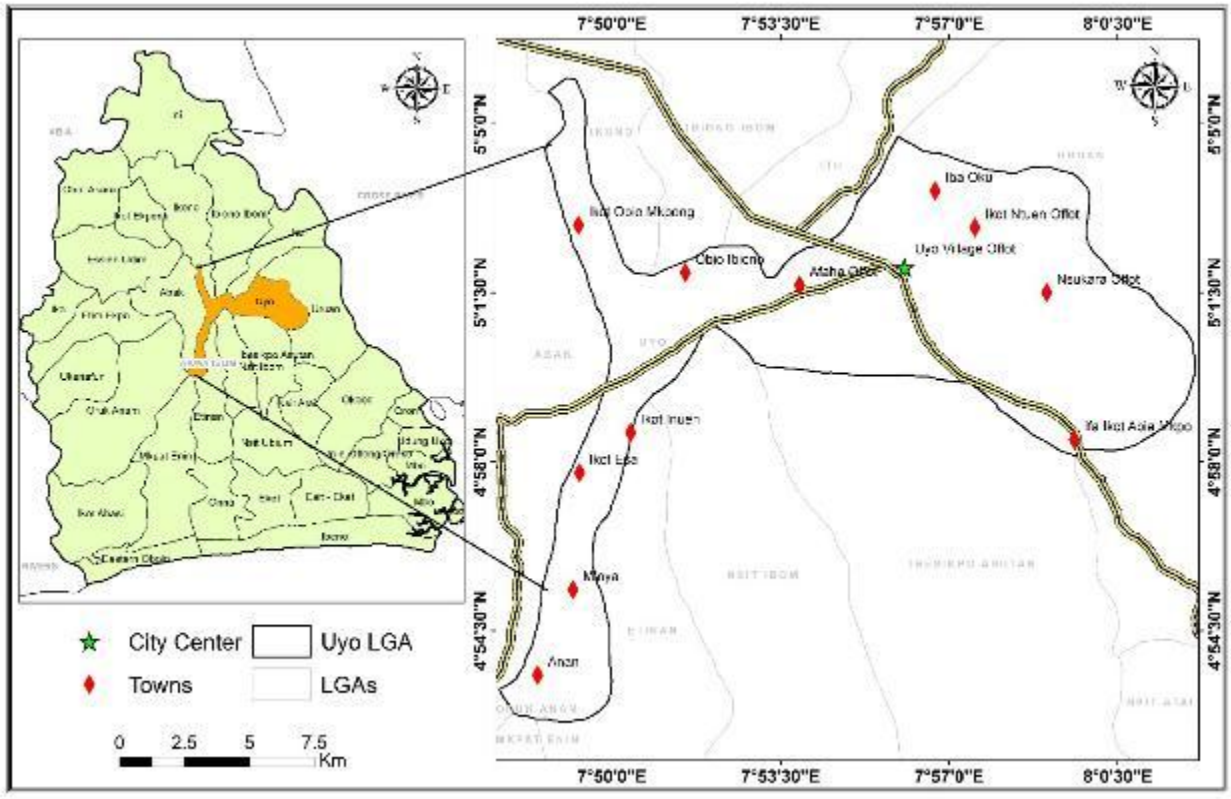



Fig 1: Location and Spatial Extent of Uyo

## Materials and Method

### Data Pre-processing

This study adopts a multi-stage experimental design involving multi-temporal satellite imagery from 2000 to 2025. The primary datasets consist of Landsat series imagery (Landsat 5 TM, 7 ETM+, and 8/9 OLI/TIRS). The selection of these specific sensors (TM, ETM+, and OLI/TIRS) ensured a continuous 25-year record of land cover change. All images were acquired during the

dry season (November–February) to minimize cloud cover interference, which is a significant constraint in tropical remote sensing.

**Table 1: Characteristics of Satellite Data (Landsat Series) Used for Multi-temporal Analysis (2000–2025)**

| Year | Sensor | Path/Row | Resolution | Source |
|---|---|---|---|---|
| 2000 | Landsat 7 ETM+ | 188/057 | 30m | USGS Earth Explorer |
| 2010 | Landsat 5 TM | 188/057 | 30m | USGS Earth Explorer |
| 2020 | Landsat 8 OLI | 188/057 | 30m | USGS Earth Explorer |
| 2025 | Landsat 9 OLI-2 | 188/057 | 30m | USGS Earth Explorer |

All images underwent rigorous preprocessing to ensure pixel-to-pixel consistency across the 25-year study period. Raw Digital Numbers (DN) were converted to Top-of-Atmosphere (TOA) reflectance to standardize the data across the varying sensors using the equation (1):

$$\rho\lambda = M_\rho \times Q_{cal} + A_\rho \qquad \text{(Eqn 1)}$$

Where: $M_\rho$ = Band Specific Multiplicative factor, $A_\rho$ = Additive factor, and $Q_{cal}$ = Digital Number (derived from the metadata document for Landsat Images (.MTL))

**Software and Computational Environment**

The implementation of the hybrid framework and geospatial analysis was conducted using a combination of open-source and industry-standard software suites:

1. Deep Learning Implementation: The Hybrid CNN-MLP model was developed using the Anaconda distribution of Python 3.12. Key libraries included TensorFlow and Keras for designing the neural network architecture, and NumPy and Pandas for handling the multi-dimensional spectral arrays.
2. Geospatial Processing: Initial image pre-processing, radiometric correction, and coordinate system transformations were performed in ArcGIS 10.5 and QGIS 3.44 Solothurn.

3. Feature Engineering: The Center-Versus-Neighbors (CVN) texture descriptors and NDVI indices were computed using the Raster Calculator and automated Python scripts within the ArcGIS environment to ensure spatial alignment with the raw spectral bands.

4. Validation: Statistical validation, including the generation of error matrices and Kappa coefficients, was performed using the Scikit-learn library.

**Model Configuration and Data Partitioning**

To ensure scientific rigor, the Hybrid CNN–MLP model was implemented within a Python 3.12 environment using TensorFlow and Keras libraries. The dataset was preprocessed into 2,499 image patches (11×11×4 input shape), partitioned into a training set of 1,749 samples and a validation set of 750 samples. The model architecture was defined as a Sequential object consisting of two Conv2D layers (32 and 64 filters) with Max-Pooling, a Flatten layer, and two Dense layers (128 and 4 units) (Table 2).

**Table 3: Hybrid CNN Model Architectural Summary**

| Layer Type | Output Shape | Parameters |
|---|---|---|
| Conv2D (32 filters) | (None, 11, 11, 32) | 1,184 |
| MaxPooling2D | (None, 5, 5, 32) | 0 |
| Conv2D (64 filters) | (None, 5, 5, 64) | 18,496 |
| MaxPooling2D | (None, 2, 2, 64) | 0 |
| Flatten | (None, 256) | 0 |
| Dense (128 units) | (None, 128) | 32,896 |
| Dropout | (None, 128) | 0 |
| Dense (4 units) | (None, 4) | 516 |

**Training Protocol:** The model was optimized using the Adam (Adaptive Moment Estimation) algorithm, chosen for its ability to compute individual adaptive learning rates and efficiently

navigate the high-dimensional spatial-spectral feature space. The model was trained over 20 epochs with a batch size optimized for the patch processing workflow. Performance was monitored through validation loss reduction, which stabilized at approximately 0.35–0.38 by the final epochs, indicating effective generalization.

**Deep MLP-CNN Hybrid Development**

A stratified random sampling approach was used to generate ground truth data for the four land-cover classes (Built-up, Vegetation, Bare Land, and Water Body). From the initial 1,200 representative points collected for each epoch, a deep learning dataset was generated comprising 2,499 image patches (11×11-pixel windows) to capture sufficient spatial context. These patches were partitioned into a training set of 1,749 samples and a validation set of 750 samples. Land Use and Land Cover (LULC) classification for the Uyo Metropolis was subsequently performed using a deep MLP-CNN Hybrid framework. The framework was developed to address the shortcomings of conventional pixel-based classification methods by combining deep learning-based spectral learning with engineered spatial contextual features. Within this architecture, the convolutional component was enhanced through feature engineering techniques designed to complement the CNN's spatial learning capability (Fig. 2). Specifically, a 3 × 3 Center-Versus-Neighbors (CVN) variability analysis (Eq 2) was applied to the Near-Infrared (NIR) band to generate a spatial variance layer capable of identifying urban edges and density variations [19].

$$CVN = \sum_{i=1}^{n} (P_i - P_c)^2 \div n \qquad (Eq\ 2)$$

Where $P_c$ = reflectance of the center pixel, $P_i$ = the values of the neighboring pixels within the moving window, n = total number of neighbors

Also, the Normalized Difference Vegetation Index (NDVI) was incorporated to introduce a biological constraint into the model, thereby improving the distinction between urban surfaces and heterogeneous vegetation cover [20]. This was computed using the expression in Equation 3.

$$NDVI = \frac{NIR - Red}{NIR + Red} \qquad (Eq\ 3)$$

For Landsat 8/9: (Band 5 – Band 4) / (Band 5 + Band 4)

JOURNAL OF SPATIAL INFORMATION SCIENCES ISSN: 2354-3361
VOL. 3, ISSUE 1, PP 34–62, 2026 DOI: https://doi.org/10.5281/zenodo.20705010
PUBLISHED 15-05-2026
www.journals.unizik.edu.ng/jsis

For Landsat 5/7: (Band 4 – Band 3) / (Band 4 + Band 3)

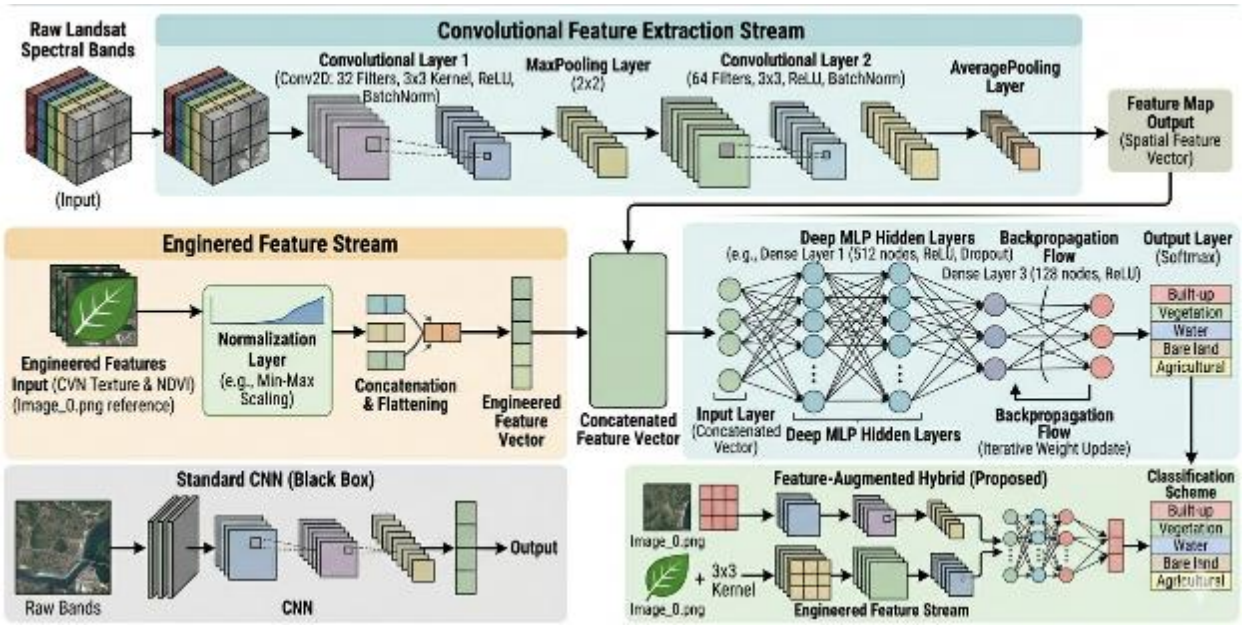



Fig 2: Difference between Standard CNN and the Hybrid CNN framework

**Post-Classification Accuracy, Comparison and Performance**

To evaluate the performance of the Deep Learning approach, the accuracy was assessed using overall accuracy and kappa statistics. Overall model accuracy was computed as:

$$OA = \frac{\sum_{i=1}^{k} n_{ii}}{N} \qquad \text{(Eq 4)}$$

Where $n_{ii}$ = correctly simulated pixels, k = number of classes, N = total number of pixels

The Kappa coefficient was used to assess agreement beyond chance using expression:

$$\varkappa = \frac{P_o - P_e}{1 - P_e} \qquad \text{(Eq 5)}$$

Where $P_o$ = observed agreement and $P_e$ = expected agreement by chance

Post-classification comparison techniques were employed to detect changes in built-up areas across the different time periods. Built-up land cover maps were extracted from each classified dataset, and change detection analysis was performed to identify areas of urban expansion, persistence, and conversion from non-built-up to built-up land uses. Spatial analysis techniques

JOURNAL OF SPATIAL INFORMATION SCIENCES ISSN: 2354-3361
VOL. 3, ISSUE 1, PP 34–62, 2026 DOI: https://doi.org/10.5281/zenodo.20705010
PUBLISHED 15-05-2026
www.journals.unizik.edu.ng/jsis

were applied to examine the magnitude, and intensity of urban growth [21]. Urban expansion was analyzed using metrics such as total built-up area, rate of expansion, and percentage change for each time interval (Table 4).

Table 4: Mathematical Formulations for Quantifying Spatiotemporal Urban Expansion Metrics.

| Spatial Measure | Expression | Description |
|---|---|---|
| Total built-up area | $A_t = N_t \times R$ | $A_t$ = total built-up area at time t (km² or ha)<br>$N_t$ = number of built-up pixels at time t<br>R = area represented by one pixel (30 m × 30 m = 900 m² in the case of Landsat) |
| Magnitude of change between two time periods | $\Delta A = A_{t_2} - A_{t_1}$ | ΔA = change in built up area and<br>$At_2$ and $At_1$ = built-up area at initial and final times |
| Rate of urban expansion | $R_e = \frac{A_{t_2} - A_{t_1}}{t_2 - t_1}$ | Re represents annual rate of urban expansion and $t_2 - t_1$ represent time interval in years |
| Percentage Change in Built-up Area | $P_c = \left(\frac{A_{t_2} - A_{t_1}}{A_{t_1}}\right) \times 100$ | $P_c$ = percentage change in built-up area |

**Presentation of Results**

**Model Performance**

An initial standalone Convolutional Neural Network (CNN) was trained to establish a baseline for deep learning performance. While the model achieved a respectable overall accuracy of 86%, a detailed analysis of the per-class metrics revealed significant limitations in Recall for bareland (0.39) and waterbody (0.35). This indicated that while the CNN identified spatial patterns effectively for dominant classes, it suffered from high omission errors in heterogeneous classes like bare soil or agricultural land.

Table 5: CNN Training Model Accuracy

JOURNAL OF SPATIAL INFORMATION SCIENCES ISSN: 2354-3361
VOL. 3, ISSUE 1, PP 34–62, 2026 DOI: https://doi.org/10.5281/zenodo.20705010
PUBLISHED 15-05-2026
www.journals.unizik.edu.ng/jsis

| LULC Class | Precision | Recall | F1-Score | Support (Samples) |
|---|---|---|---|---|
| Built ups | 0.93 | 0.96 | 0.94 | 220 |
| Vegetation | 0.84 | 0.99 | 0.91 | 377 |
| Bareland | 0.75 | 0.39 | 0.52 | 127 |
| Waterbody | 1.00 | 0.35 | 0.51 | 26 |
| Overall Accuracy | | | 0.86 | 750 |
| Macro Average | 0.88 | 0.67 | 0.72 | 750 |
| Weighted Average | 0.86 | 0.86 | 0.84 | 750 |

The CNN model demonstrated steady convergence during training, with training accuracy increasing from 39.42% in Epoch 1 to 88.03% in Epoch 20. Similarly, validation accuracy improved from 50.27% to 86.00%, indicating good generalization performance on unseen data. Concurrently, training loss decreased from 1.2463 to 0.3381, while validation loss declined from 1.0593 to 0.3468, confirming effective learning and model optimization. The highest validation accuracy (86.40%) was achieved at Epoch 19, while the lowest validation loss (0.3468) occurred at Epoch 20, suggesting that the model had nearly converged with minimal overfitting (Table 6).

Table 6: Key Performance Indicators from CNN Model

| Metric | Value |
|---|---|
| Initial Training Accuracy | 39.42% |
| Final Training Accuracy | 88.03% |
| Initial Validation Accuracy | 50.27% |
| Final Validation Accuracy | 86.00% |
| Initial Training Loss | 1.2463 |
| Final Training Loss | 0.3381 |

| | |
|---|---|
| Initial Validation Loss | 1.0593 |
| Final Validation Loss | 0.3468 |
| Best Validation Accuracy | 86.40% (Epoch 19) |
| Lowest Validation Loss | 0.3468 (Epoch 20) |

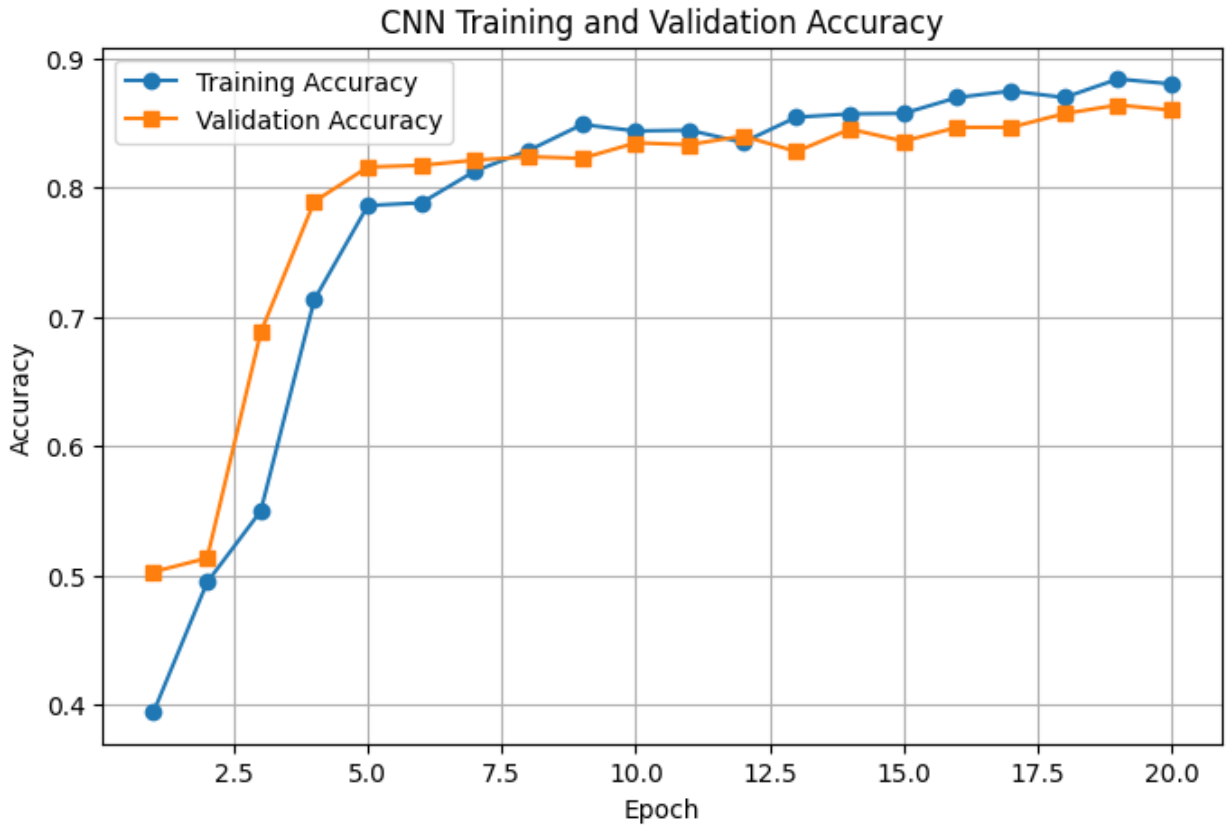



**Figure 3.** Training and validation accuracy curves of the Convolutional Neural Network (CNN) model over 20 training epochs. The graph illustrates the progressive improvement in classification performance during model training and evaluation on the validation dataset.

As shown in Figure 3, both training and validation accuracies increased consistently throughout the training process, indicating effective learning by the CNN model. The training accuracy

improved from 39.42% in the first epoch to 88.03% by the twentieth epoch, while validation accuracy increased from 50.27% to 86.00% over the same period. A rapid increase in accuracy was observed during the initial epochs, particularly between Epochs 3 and 8, suggesting that the model quickly learned the discriminative features necessary for classification. Beyond Epoch 10, the accuracy curves began to stabilize, indicating convergence of the learning process. The relatively small gap between the training and validation accuracy curves demonstrates good generalization capability and suggests that the model did not suffer from significant overfitting. The highest validation accuracy of 86.40% was achieved at Epoch 19, confirming the effectiveness of the CNN architecture in accurately classifying the input data.

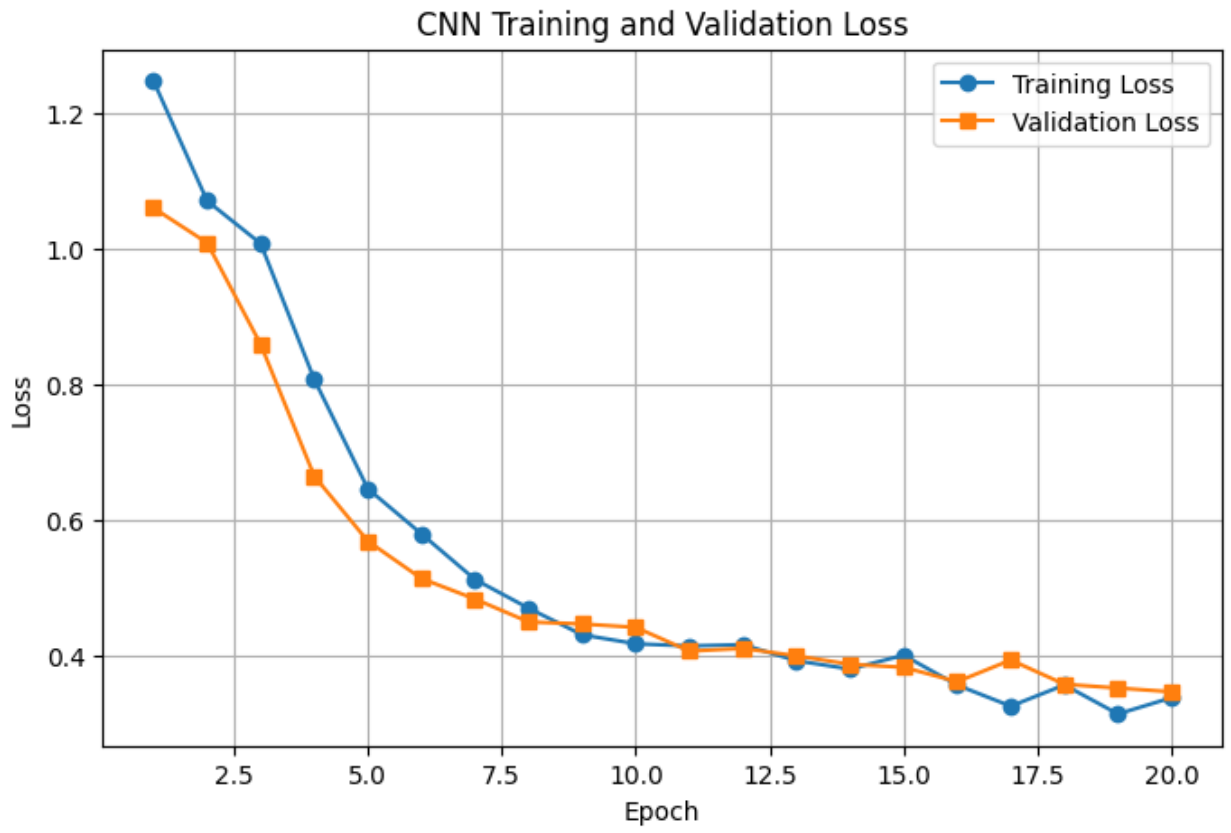



Figure 4: Training and validation loss curves of the Convolutional Neural Network (CNN) model over 20 training epochs. The graph depicts the reduction in prediction error as the model progressively learns representative features from the training data.

Figure 4 demonstrated a steady decline in both training and validation loss values throughout the training process, indicating successful optimization of the CNN model. Training loss decreased substantially from 1.2463 in Epoch 1 to 0.3381 in Epoch 20, while validation loss declined from 1.0593 to 0.3468. The sharp reduction in loss during the early epochs reflects rapid feature learning and parameter adjustment by the network. After approximately Epoch 10, the loss curves exhibited a more gradual decline, suggesting that the model was approaching convergence. Although minor fluctuations were observed in the validation loss, particularly around Epochs 15–17, the overall downward trend indicates stable learning and effective generalization. The lowest validation loss recorded at Epoch 20 further confirms that the model achieved an optimal balance between fitting the training data and maintaining predictive performance on unseen samples.

**Classification Accuracy**

The model was applied to classify Landsat imagery for the years 2020 and 2025 in order to evaluate its consistency, robustness, and temporal performance in land cover classification. For the 2020 Landsat image, the model achieved an overall classification accuracy of 93.09%, with training and testing RMS errors of 0.1502 and 0.1479, respectively. The close agreement between these RMS values indicates good generalization capability and minimal overfitting. The overall skill measure of 0.9136 further confirmed strong predictive performance beyond random classification. In comparison, the 2025 Landsat image classification exhibited improved model performance. The overall accuracy increased to 95.04%, while training and testing RMS errors decreased to 0.1254 and 0.1274, respectively. This reduction in error values suggested enhanced learning efficiency and improved feature separability in the 2025 dataset. The higher overall skill measure of 0.9380 indicated superior classification reliability relative to the 2020 results.

The Hybrid CNN-MLP framework demonstrated superior performance across all four epochs (2000, 2010, 2020, and 2025). The model achieved an Overall Accuracy (OA) of 96.17% and a Kappa Coefficient of 0.94 for the 2025 classification (Table 7). In contrast, the traditional Maximum Likelihood Classifier (MLC) struggled significantly, particularly in the 2010 and 2020 datasets, where accuracies hovered between 67% and 78% [22].

**Table 7: Comparative Classification Accuracy Metrics for the Hybrid CNN–MLP Framework (2000–2025).**

| Year | Overall Accuracy (%) | Kappa Statistic | Built-up UA (%) | Bareland UA (%) |
|---|---|---|---|---|
| 2000 | 94.23 | 0.916 | 98.12 | 90.12 |
| 2010 | 94.01 | 0.911 | 96.91 | 84.40 |
| 2020 | 93.95 | 0.910 | 98.70 | 79.19 |
| 2025 | 96.17 | 0.942 | 98.64 | 91.45 |

The comparative accuracy assessment indicated consistently strong classification performance across all study years, with overall accuracies above 93% and Kappa statistics exceeding 0.90. The Built-up class achieved very high User's Accuracy values throughout the study period, ranging from 96.91% to 98.70%, demonstrating the effectiveness of the hybrid CNN–MLP framework in identifying urban features. In contrast, the Bareland class showed comparatively lower accuracies, particularly in 2020 (79.19%), reflecting persistent spectral confusion between bare surfaces and built-up areas within the heterogeneous tropical environment [23]. Nevertheless, the improvement observed in 2025 suggests enhanced class separability and improved model generalization [17].

**Resolution of Spectral Confusion**

Traditional classifiers often struggled with spectral confusion (where Bareland and Built-up areas have identical reflectance). Within the Hybrid CNN-MLP framework, the model successfully distinguished the 'rough' texture of urban rooftops from the 'smooth' texture of bare land, resulting in a significantly lower Error of Commission for the Built-up class (1.3% in 2020 and 1.36% in 2025). Class-based skill analysis revealed a consistent performance pattern across both years. For 2020, built ups and vegetation classes recorded very high skill measures of 0.9726 and 0.9442, respectively, indicating excellent class discrimination.

Agricultural land (0.8699) and bareland (0.8071) also demonstrated satisfactory predictive skill, though with slightly reduced performance likely due to spectral overlap or transitional land cover characteristics [24]. Similarly, the 2025 classification showed strong improvement across the first

JOURNAL OF SPATIAL INFORMATION SCIENCES ISSN: 2354-3361
VOL. 3, ISSUE 1, PP 34–62, 2026 DOI: https://doi.org/10.5281/zenodo.20705010
PUBLISHED 15-05-2026
www.journals.unizik.edu.ng/jsis

four classes. Skill values increased to 0.9899 (built ups), 0.9670 (vegetation), 0.9002 (agricultural land), and 0.8446 (bareland), reflecting enhanced separability and model learning. These results indicate that the neural network consistently identified dominant land cover classes with high reliability across both years.

**Comparative Analysis and Performance Validation**

To validate the efficiency of the proposed Hybrid CNN–MLP framework, a comparative performance analysis was conducted against traditional machine learning baselines, specifically Random Forest (RF) (Fig 5 and 6). These classifiers were trained using the same 1,749 training samples and evaluated on the same 750-sample validation set.

Table 8: Comparative Performance Analysis: Random Forest Baseline vs. Proposed Hybrid CNN-MLP Framework

| Model | Overall Accuracy (OA) | Kappa Coefficient | Training Time (min) |
|---|---|---|---|
| Random Forest (RF) | 82.4% | 0.78 | 12.5 |
| Proposed Hybrid CNN-MLP | 96.17% | 0.94 | 18.4 |

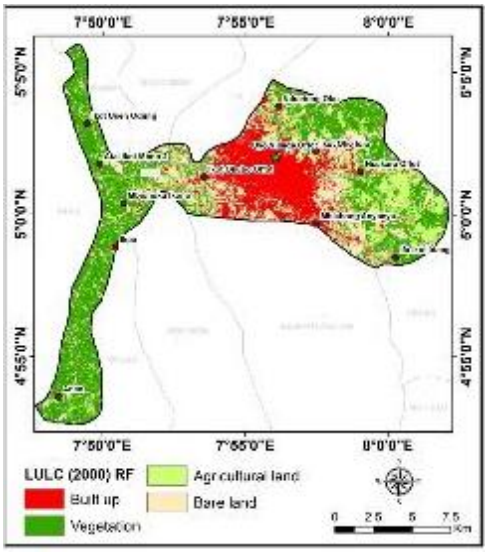



Fig 5: Land Use Classification Using Random Forest Algorithm (Year 2000)

JOURNAL OF SPATIAL INFORMATION SCIENCES ISSN: 2354-3361
VOL. 3, ISSUE 1, PP 34–62, 2026 DOI: https://doi.org/10.5281/zenodo.20705010
PUBLISHED 15-05-2026
www.journals.unizik.edu.ng/jsis

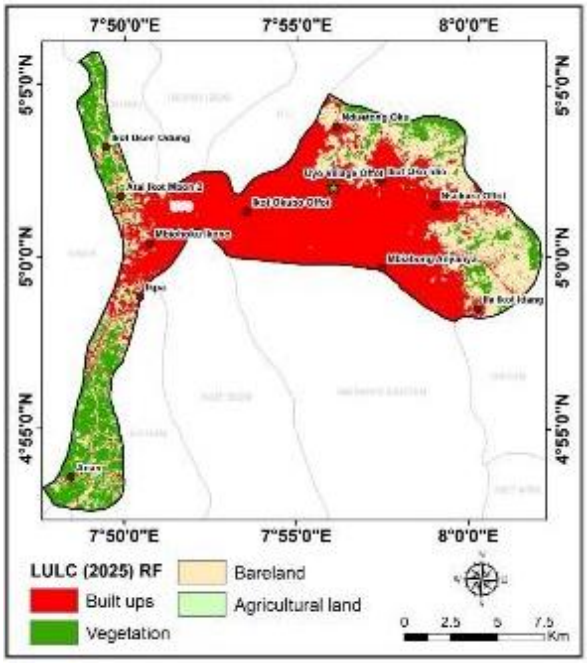



Fig 6: LULC Classification Using RF (2025)

The results demonstrated that while Random Forest provide acceptable baseline accuracy, they struggle to resolve spectral confusion between high-albedo concrete rooftops and bare sandy surfaces. The Hybrid CNN-MLP framework outperformed the RF model by approximately 14% in Overall Accuracy (Table 8). This significant margin is attributed to the dual-stream processing capability: the CNN component successfully extracted spatial contextual patterns (edges and morphological structures), while the MLP component optimized the non-linear spectral signatures. The inclusion of the Center-Versus-Neighbors (CVN) texture descriptor was essential in this performance gain, providing the necessary spatial variance context that pixel-based RF algorithms lack. This confirmed that the integrated approach is not only statistically superior but also robust against the spectral confusion phenomenon common in tropical urban landscapes.

## Spatiotemporal LULC Dynamics (2000–2025)

### *Analysis of Land Cover Transitions*

The classification results reveal a dramatic reorganization of Uyo's spatial structure over the 25-year study period. The most salient feature of this transformation is the aggressive expansion of Built-up Areas, which grew from 36.51 km² (19.89%) in 2000 to 94.24 km² (51.34%) by 2025. This represents a total increase of 158.10%, signaling the transition of Uyo from a regional administrative center into a major urban metropolis. Conversely, the "natural" land covers

experienced significant volatility and decline. Vegetation, while showing a slight recovery in the final epoch due to successful classification of peri-urban fallow lands, dropped from a dominant 53.27% in 2000 to approximately 38.27% in 2025. The Bare Land category showed a consistent downward trend, decreasing from 29.56 km² to 7.98 km² (Table 9). This decline is technically significant; it suggests that "speculative bare land" (land cleared for development) was rapidly converted into permanent structures, a transition precisely captured by the model's texture analysis [17].

Table 9: Land Use/Land Cover (LULC) Class Distribution and Decadal Changes in Uyo Metropolis (2000–2025).

| **Land Use/Land Cover** | **2000 Area (sq km)** | **2000 (%)** | **2010 Area (sq km)** | **2010 (%)** | **2020 Area (sq km)** | **2020 (%)** | **2025 Area (sq km)** | **2025 (%)** |
|---|---|---|---|---|---|---|---|---|
| Built-up Areas | 36.51 | 19.89 | 72.94 | 39.73 | 74.48 | 40.58 | 94.24 | 51.34 |
| Vegetation | 97.78 | 53.27 | 70.10 | 38.19 | 45.37 | 24.72 | 70.25 | 38.27 |
| Agricultural Land | 19.71 | 10.74 | 14.10 | 7.68 | 47.04 | 25.63 | 11.08 | 6.04 |
| Bare Land | 29.56 | 16.10 | 26.43 | 14.40 | 16.67 | 9.08 | 7.98 | 4.35 |
| **Total** | **183.56** | **100** | **183.56** | **100** | **183.56** | **100** | **183.56** | **100** |

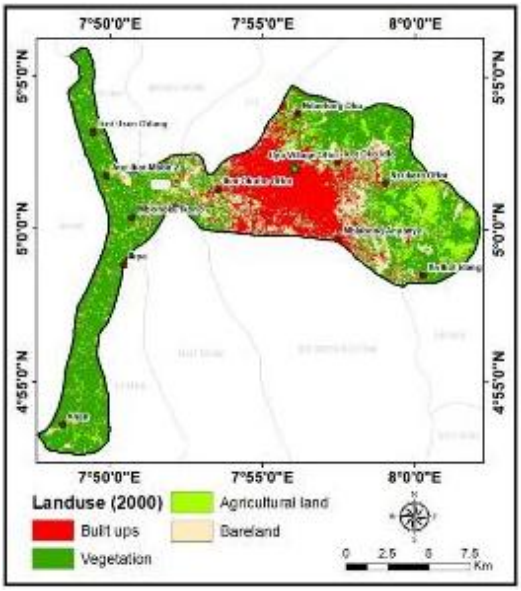



Fig 7: Land use classification for Uyo (Year 2000)

JOURNAL OF SPATIAL INFORMATION SCIENCES ISSN: 2354-3361
VOL. 3, ISSUE 1, PP 34–62, 2026 DOI: https://doi.org/10.5281/zenodo.20705010
PUBLISHED 15-05-2026
www.journals.unizik.edu.ng/jsis

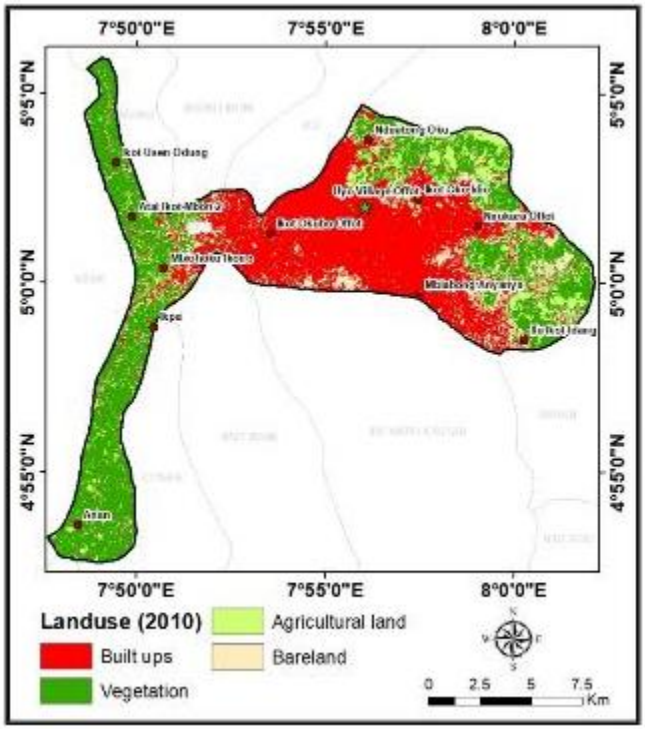



Fig 8: Land use classification for Uyo (Year 2010)

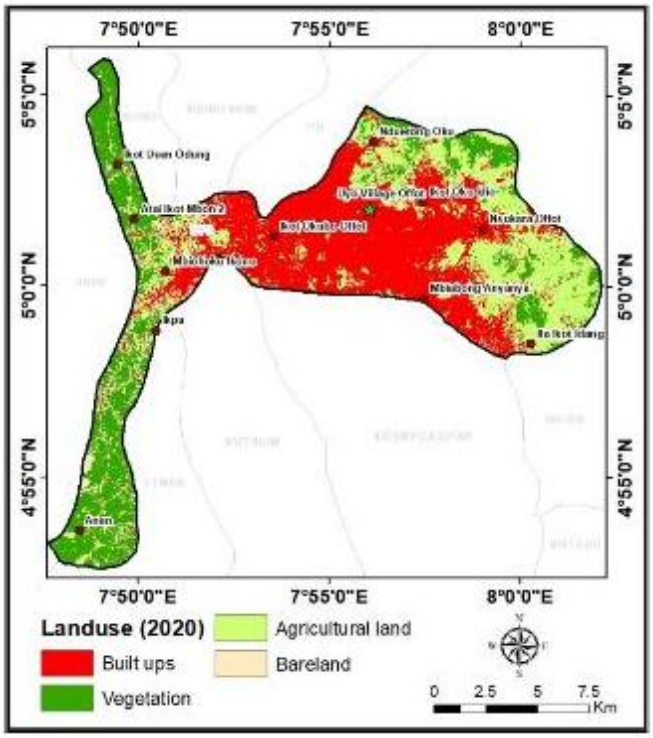



Fig 9: Land use classification for Uyo (Year 2020)

JOURNAL OF SPATIAL INFORMATION SCIENCES ISSN: 2354-3361
VOL. 3, ISSUE 1, PP 34–62, 2026 DOI: https://doi.org/10.5281/zenodo.20705010
PUBLISHED 15-05-2026
www.journals.unizik.edu.ng/jsis

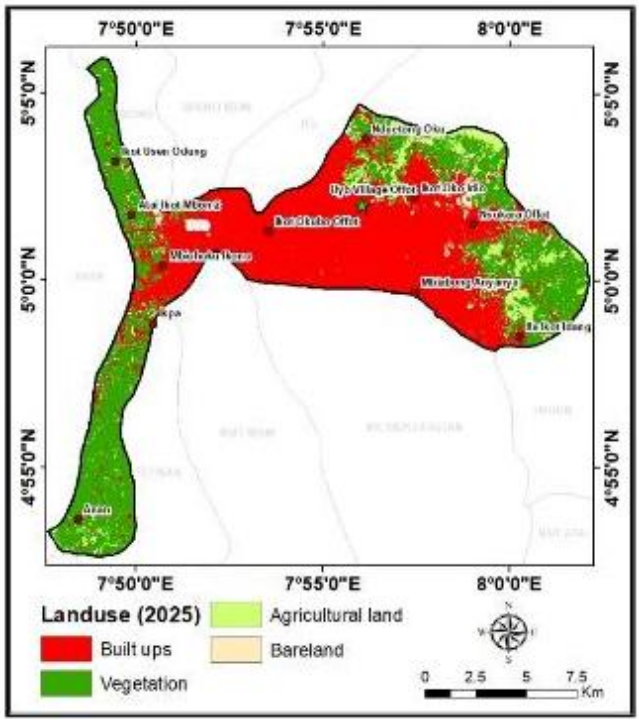



Fig 10: Land use classification for Uyo (Year 2025)

***Quantitative Analysis of Urban Expansion Rates***

The pace of urban growth in Uyo was not linear, as evidenced by the varying rates of expansion across the three intervals (Table 10):

i. 2000–2010 (The Rapid Boom): This decade saw the highest percentage growth (99.75%), with an expansion rate of 3.64 km²/year. This coincides with the post-democratic transition period and heavy state-led infrastructural investment in the capital.

ii. 2010–2020 (The Consolidation Phase): Growth significantly slowed to 0.15 km²/year. This phase represents "infilling" where development occurred within existing urban boundaries rather than outward expansion.

iii. 2020–2025 (The Modern Surge): The current interval shows a renewed surge in expansion, reaching its highest recorded rate of 3.95 km²/year. This recent spike underscores the necessity of the high-accuracy Hybrid CNN-MLP model to monitor rapid, real-time changes in the urban fringe.

JOURNAL OF SPATIAL INFORMATION SCIENCES ISSN: 2354-3361
VOL. 3, ISSUE 1, PP 34–62, 2026 DOI: https://doi.org/10.5281/zenodo.20705010
PUBLISHED 15-05-2026
www.journals.unizik.edu.ng/jsis

Table 10: Quantitative Analysis of Urban Growth

| Interval | Initial Area (Δt1) | Final Area (Δt2) | Magnitude of Change (ΔA) | Rate of Expansion ($R_e$) | Percentage Change (Pc) |
|---|---|---|---|---|---|
| **2000–2010** | 36.51 | 72.94 | 36.42 | 3.64 km²/year | 99.75% |
| **2010–2020** | 72.94 | 74.48 | 1.55 | 0.15 km²/year | 2.12% |
| **2020–2025** | 74.48 | 94.24 | 19.76 | 3.95 km²/year | 26.53% |
| **2000–2025 (Total)** | 36.51 | 94.24 | 57.73 | 2.31 km²/year | 158.10% |

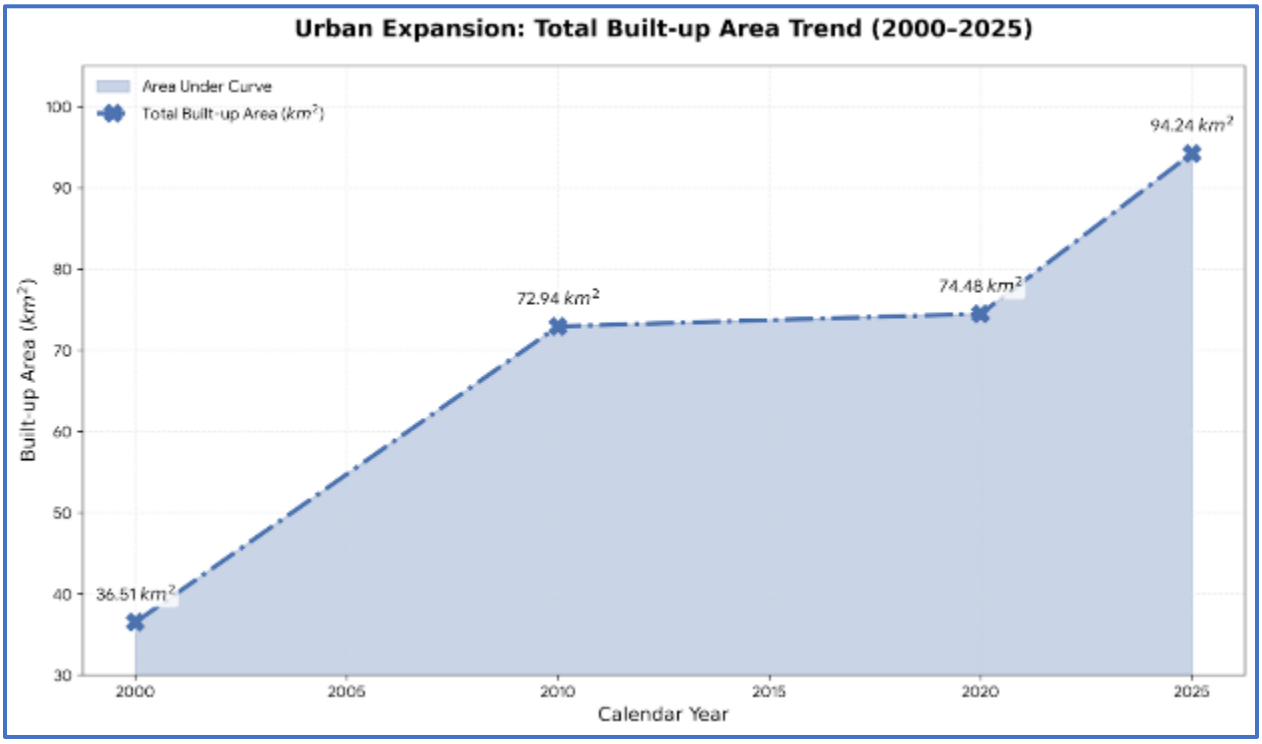



Fig 11: Upward Trend of Urban Expansion (2000 – 2025)

The ability of the framework to maintain an overall accuracy of 96.17% despite these rapid shifts is noteworthy. Traditional classifiers often struggle during "surge" periods (like 2020–2025)

because the spectral signatures of active construction sites (Bare Land) and completed buildings (Built-up) are remarkably similar [25]. The findings confirm that the inclusion of CVN Texture allowed the model to correctly categorize the 19.76 km² of new built-up area added in the last five years without misclassifying it as bare soil.

**Discussion**

The findings demonstrate that integrating expert-derived spatial features with deep learning significantly improves Land Use and Land Cover (LULC) classification in heterogeneous tropical urban environments. The Hybrid CNN–MLP framework achieved an overall classification accuracy of 96.17%, substantially outperforming the RF Classifier (84.20%). This improvement showed the importance of combining spatial-textural information with spectral data when classifying complex urban landscapes. The result supports previous studies that emphasize the superiority of hybrid deep learning architectures for resolving spectral ambiguities in remotely sensed imagery [26] [27]. Unlike conventional pixel-based approaches that rely primarily on spectral signatures, the proposed framework used Center-Versus-Neighbors (CVN) texture descriptors and NDVI-derived information to capture both contextual and spectral characteristics of land-cover classes. Consequently, the model was better able to distinguish between spectrally similar surfaces such as bare soil, construction sites, and built-up areas, which are common sources of classification error in tropical cities [28].

The high classification performance obtained in this study further demonstrates the value of incorporating spatial intelligence into medium-resolution satellite imagery. Previous research has shown that convolutional neural networks can effectively learn spatial patterns from remotely sensed data, thereby reducing the limitations associated with traditional machine learning classifiers [12]. The present findings extend this understanding by showing that expert-engineered texture features can complement deep learning architectures and enhance their ability to characterize urban morphology using freely available Landsat imagery. This is particularly important for developing countries where access to high-resolution commercial imagery may be limited by financial and technical constraints [14]. The results therefore suggest that reliable urban monitoring can be achieved using cost-effective datasets when combined with appropriate feature extraction and deep learning techniques.

Beyond methodological improvements, the study provides important insights into the urban growth dynamics of Uyo Metropolis. The analysis revealed a substantial increase in built-up area between 2000 and 2025, amounting to approximately 158.10%. This pattern reflects the rapid urbanization processes occurring across many secondary cities in sub-Saharan Africa, where population growth, infrastructure development, and economic expansion are driving significant land transformation. Similar patterns of urban expansion have been reported in other rapidly growing cities, including Cotonou and several tropical urban centres, where built-up development has increasingly encroached upon vegetation and agricultural land [29] [30]. The ability of the proposed hybrid model to accurately separate newly developed surfaces from bare land was particularly important for quantifying these changes, as these classes frequently exhibit similar spectral characteristics and are often confused in conventional classification approaches.

The temporal analysis also revealed distinct phases of urban development. A period of rapid expansion between 2000 and 2010 was followed by relatively slow outward growth during 2010–2020, before a renewed acceleration in urban expansion occurred between 2020 and 2025. This pattern is consistent with the urban "infilling and sprawl" framework described in urban geography literature [30] [31]. The reduced rate of expansion during the intermediate period may indicate that development activities were concentrated within existing urban boundaries through densification and infilling processes. In contrast, the sharp increase observed after 2020 suggests renewed outward expansion into previously undeveloped areas. Such trends have important implications for sustainable urban planning, as continued outward growth may increase pressure on surrounding vegetation, agricultural land, and ecosystem services if not effectively managed.

**Conclusion**

This study successfully developed and implemented a Hybrid CNN-MLP Deep Learning framework to monitor the rapid spatiotemporal dynamics of Uyo, Nigeria, from 2000 to 2025. By integrating CVN Texture and NDVI, the hybrid model achieved a superior overall accuracy of 96.17%, effectively resolving the long-standing spectral confusion between built-up areas and bare land. The findings revealed a massive 158.10% increase in urban footprint over 25 years, characterized by a transition from administrative core growth to aggressive peri-urban sprawl. The

model's ability to capture these non-linear growth patterns, including the recent "surge" between 2020 and 2025, demonstrates its robustness as a high-precision monitoring tool.

It is recommended that state planning authorities, such as the Akwa Ibom State Ministry of Lands and Housing, transition from traditional manual mapping to automated Deep Learning frameworks. This could support near real-time monitoring of unauthorized urban expansion and better infrastructure targeting. Future research should explore the integration of additional spatial descriptors, such as Synthetic Aperture Radar (SAR) data, to further enhance classification accuracy during the tropical cloud-cover seasons. Also, the high-accuracy maps produced by this model can serve as the baseline for calculating Land Use Efficiency (LUE) metrics, ensuring that Uyo's expansion remains aligned with Sustainable Development Goal (SDG) 11 targets.

**References**

[1] Ukpo, E., Eyoh, A., Nwilag, B., & Department. (2025). Geographically Weighted Regression and Ordinary Least Squares in Assessing Urban Growth; A Case Study of Uyo Metropolis, Nigeria. International Journal Of Research And Innovation In Applied Science, X(VIII), 95–109. https://doi.org/10.51584/IJRIAS.2025.100800007

[2] Essien, E. (2022). Impacts of Governance Toward Sustainable Urbanization in a Midsized City: A Case Study of Uyo, Nigeria. Land, 11(1). https://doi.org/10.3390/land11010037

[3] Latif, R. M. A., Arshad, A., He, J., Ahmad, T., & Ahmed, A. (2025). Geospatial Modeling and Forecasting of Urban Land Use Change Using Google Earth Engine And Machine Learning. Plos One, 20(12 December), 1–24. https://doi.org/10.1371/journal.pone.0338920

[4] Rayeen, M. S., Usmani, T. M., & Rahman, A. (2026). Quantifying the Impact of Land Use and Land Cover Change on Land Surface Temperature using Spatiotemporal Multispectral Remote Sensing Data. Discover Environment, 4(36), 1–28. https://doi.org/10.1007/s44274-026-00537-2

[5] Hester, D. B., Cakir, H. I., Nelson, S. A. C., & Khorram, S. (2008). Per-pixel Classification of High Spatial Resolution Satellite Imagery for Urban Land-Cover Mapping.

Photogrammetric Engineering and Remote Sensing, 74(4), 463–471. https://doi.org/10.14358/PERS.74.4.463

[6] Gui, B., Sam, L., Bhardwaj, A., Gómez, D. S., Peñaloza, F. G., Buchroithner, M. F., & Green, D. R. (2025). Optimizing Object-Based Agricultural and Ecological Land Use Classification Via Multi-Band Fusion and Seasonal Spectral Differences. International Journal of Remote Sensing, 46(16), 6157–6188. https://doi.org/10.1080/01431161.2025.2532837

[7] Mancino, G., Falciano, A., Console, R., & Trivigno, M. L. (2023). Comparison between Parametric and Non-Parametric Supervised Land Cover Classifications of Sentinel-2 MSI and Landsat-8 OLI Data. Geographies, 3(1), 82–109. https://doi.org/10.3390/geographies3010005

[8] Yaro, H., Aliyu, N., Babayo, J. A., Atang, I., Ezekiel, E., Jimmy, D., Samanja, R. E., & Flourish, O. A. (2025). Examining Deforestation and Forest Degradation in North-Eastern Nigeria. International Journal of Scientific Research and Modern Technology, 4(3), 43–53. https://doi.org/10.38124/ijsrmt.v4i3.349

[9] Mahmoud, A. S., Mezaal, M. R., Hameed, M. R., & Naje, A. S. (2022). A Framework for Improving Urban Land Cover Using Object and Pixel-Based Techniques via Remotely Sensed Data. Nature Environment and Pollution Technology, 21(5), 2189–2200. https://doi.org/10.46488/NEPT.2022.v21i05.013

[10] Boulila, W., Ghandorh, H., Khan, M. A., Ahmed, F., & Ahmad, J. (2021). A Novel CNN-LSTM-Based Approach to Predict Urban Expansion. Ecological Informatics, 64, 1–24. https://doi.org/10.1016/j.ecoinf.2021.101325

[11] Çiklaçandir, F. G. Y., & Utku, S. (2023). Performance Comparison of CNN Based Hybrid Systems Using UC Merced Land-Use Dataset. Deu Muhendislik Fakultesi Fen ve Muhendislik, 25(75), 725–737. https://doi.org/10.21205/deufmd.2023257516

[12] Ali, K., & Johnson, B. (2022). Land-Use and Land-Cover Classification in Semi-Arid Areas from Medium-Resolution Remote-Sensing Imagery: A Deep Learning Approach. Sensors (Basel, Switzerland), 22. https://doi.org/10.3390/s22228750.

[13] Naushad, R., Kaur, T., & Ghaderpour, E. (2021). Deep Transfer Learning for Land Use and Land Cover Classification: A Comparative Study. Sensors (Basel, Switzerland), 21. https://doi.org/10.3390/s21238083.

[14] Shawky, O. A., Hagag, A., El-Dahshan, E. S. A., & Ismail, M. A. (2020). Remote Sensing Image Scene Classification using CNN-MLP with Data Augmentation. Optik, 221(June), 165356. https://doi.org/10.1016/j.ijleo.2020.165356

[15] Zhang, C., Pan, X., Li, H., Gardiner, A., Sargent, I., Hare, J., & Atkinson, P. M. (2018). A Hybrid MLP-CNN Classifier for Very Fine Resolution Remotely Sensed Image Classification. ISPRS Journal of Photogrammetry and Remote Sensing, 140, 133–144. https://doi.org/10.1016/j.isprsjprs.2017.07.014

[16] Wambugu, N., Chen, Y., Xiao, Z., Wei, M., Bello, S., M., J., & Li, J. (2021). A Hybrid Deep Convolutional Neural Network for Accurate Land Cover Classification. Int. J. Appl. Earth Obs. Geoinformation, 103, 102515. https://doi.org/10.1016/j.jag.2021.102515.

[17] Essien, E., & Cyrus, S. (2019). Detection of Urban Development in Uyo (Nigeria) using Remote Sensing. Land, 8(6), 1–13. https://doi.org/10.3390/LAND8060102

[18] Essien, E., & Samimi, C. (2021). Evaluation Of Economic Linkage Between Urban Built-Up Areas in a Mid-Sized City Of Uyo (Nigeria). Land, 10(10). https://doi.org/10.3390/land10101094

[19] Mahmoudzadeh, H., Abedini, A., & Aram, F. (2022). Urban Growth Modeling and Land-Use/Land-Cover Change Analysis in a Metropolitan Area (Case Study: Tabriz). Land, 11(12). https://doi.org/10.3390/land11122162

[20] Tong, X. Y., Xia, G. S., Lu, Q., Shen, H., Li, S., You, S., & Zhang, L. (2020). Land-cover Classification with High-Resolution Remote Sensing Images using Transferable Deep Models. Remote Sensing of Environment, 237, 1–35. https://doi.org/10.1016/j.rse.2019.111322

[21] Alegbeleye, O. M., Rotimi, Y. O., Shomide, P., Oyediran, A., Ogundipe, O., & Akintunde-Alo, A. (2024). Land use land cover (LULC) Analysis in Nigeria: A Systematic Review of Data, Methods, And Platforms With Future Prospects. Bulletin of the National Research Centre, 48(1). https://doi.org/10.1186/s42269-024-01286-z

[22] Rawat, K. S., Kumar, S., & Garg, N. (2024). Statistical Comparison of Simple and Machine Learning Based Land Use and Land Cover Classification Algorithms: A case study. Journal of Water Management Modeling, 32. https://doi.org/10.14796/JWMM.H524

[23] Fayaz, M., Nam, J., Dang, L. M., Song, H., & Moon, H. (2024). Land-Cover Classification Using Deep Learning with High-Resolution Remote-Sensing Imagery. Appl. Sci, 14, 1–15. https://doi.org/10.3390/app14051844

[24] Din, S. U., & Mak, H. W. L. (2021). Retrieval Of Land-Use/Land Cover Change (LUCC) Maps And Urban Expansion Dynamics of Hyderabad, Pakistan Via Landsat Datasets And Support Vector Machine Framework. Remote Sensing, 13(16), 1–25. https://doi.org/10.3390/rs13163337

[25] Liu, S., Zhang, J., Wang, L., Ciais, P., Zhang, J., Penuelas, J., Nath, B., Jacquet, I., Wu, X., Ding, S., Li, W., Huang, N., Song, W., Ni, W. J., & Niu, Z. (2025). Mapping Previously Undetected Trees Reveals Overlooked Changes In Pan-Tropical Tree Cover. Nature Communications, 16(1). https://doi.org/10.1038/s41467-025-60662-z

[26] Zhang, C., Sargent, I., Pan, X., Li, H., Gardiner, A., Hare, J., & Atkinson, P. M. (2019). Joint Deep Learning for Land Cover and Land Use Classification. Remote Sensing of Environment, 221, 173–187. https://doi.org/10.1016/j.rse.2018.11.014

[27] Zhu, Y., Geiß, C., So, E., Bardhan, R., Taubenböck, H., & Jin, Y. (2024). Urban expansion simulation with an explainable ensemble deep learning framework. Heliyon, 10(7). https://doi.org/10.1016/j.heliyon.2024.e28318

[28] Tadesa Edosa, B., Geleta Erena, M., Nagasa Wolteji, B., Tolossa Werati, G., & Dangia Nagasa, M. (2024). Urban growth assessment using machine learning algorithms, GIS techniques, and its impact on biodiversity: The case of Sululta sub-city, Central Oromia, Ethiopia. City and Environment Interactions, 23(May), 100151. https://doi.org/10.1016/j.cacint.2024.100151

[29] Ahouandjinou, S. D. I T. K., Sodalo, C., Sambieni, R. K., Osseni, A. A., Akossou, A. Y. J., & Bogaert, J. (2025). Built-up Expansion and Urban Land Use Trade-Offs in Peri-Urban Cotonou (Benin), West Africa: A Scenario-Based Remote Sensing Approach. City

and Environment Interactions, 28(November), 1–12. https://doi.org/10.1016/j.cacint.2025.100263

[30] Khan, D., Khan, N., Choudhury, U., Singh, S. K., Kanga, S., Kumar, P., & Meraj, G. (2025). Urban Expansion and Spatial Growth Patterns in Lucknow: Implications for Sustainable Development (1991–2021). Sustainability (Switzerland), 17(1). https://doi.org/10.3390/su17010227

[31] Yasin, M. Y., Yusoff, M. M., Abdullah, J., Noor, N. M., & Noor, N. M. (2021). Urban Sprawl Literature Review: Definition and Driving Force. Malaysian Journal of Society and Space, 17(2), 116–128. https://doi.org/10.17576/geo-2021-1702-10